

Study of an $S = 1$ Ni^{II} pincer electrocatalyst precursor for aqueous hydrogen production based on paramagnetic ¹H NMR†

Cite this: *Dalton Trans.*, 2013, **42**, 8802Oana R. Luca,^a Steven J. Konezny,^{*a,b} Eric K. Paulson,^a Fatemah Habib,^{c,d} Kurt M. Luthy,^a Muralee Murugesu,^{c,d} Robert H. Crabtree^{*a,b} and Victor S. Batista^{*a,b}

A tridentate NNN Ni^{II} complex, shown to be an electrocatalyst for aqueous H₂ production at low overpotentials, is studied by using temperature-dependent paramagnetic ¹H NMR. The NMR T₁ relaxation rates, temperature dependence of the chemical shifts, and dc SQUID magnetic susceptibility are correlated to DFT chemical shifts and compared with the properties of a diamagnetic Zn analogue complex. The resulting characterization provides an unambiguous assignment of the six proton environments in the meridionally coordinating tridentate NNN ligand. The demonstrated NMR/DFT methodology should be valuable in the search for appropriate ligands to optimize the reactivity of 3d metal complexes bound to attract increasing attention in catalytic applications.

Received 27th February 2013,
Accepted 14th April 2013

DOI: 10.1039/c3dt50528f

www.rsc.org/dalton

Introduction

Understanding the nature of electrocatalytic pincer complexes based on earth-abundant 3d transition metals is a subject of great current interest due to the wide range of possible applications, including catalysis for hydrogen production and storage.^{1,2} Structure–activity relationships are fundamental to catalyst optimization. However, characterization is often challenging due to the substitutional lability and paramagnetism typical of 3d transition metal complexes. Therefore, there is an urgent need to establish methodologies for this general class of catalysts. NMR spectroscopy is a prime means of identifying and characterizing diamagnetic precatalysts, and potential catalytic intermediates. Extension to paramagnetic 3d metal complexes remains underutilized because of the difficulties in signal assignment and interpretation of the NMR spectra.^{3,4} Here, we apply paramagnetic ¹H NMR spectroscopy in solution to analyze a Ni^{II}NNN complex (Fig. 1) that was recently shown

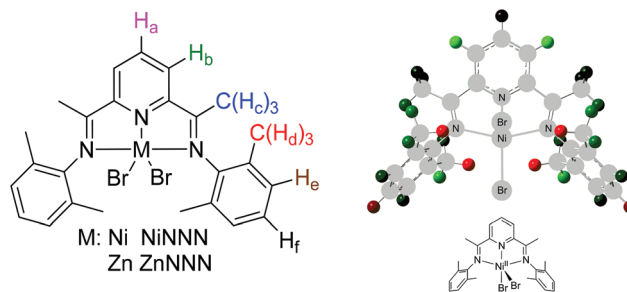


Fig. 1 Proton labeling for the NiNNN and ZnNNN complexes (left) and spin populations of the NiNNN complex (right) calculated at the DFT UB3LYP/6-311++G(d,p) level of theory (excess α and β spin densities are shown on the right in green (e.g., H_b) and red (e.g., H_d), respectively).

to be an effective electrocatalyst for proton reduction under aqueous conditions.^{2a} The diamagnetic reference shift, necessary for the analysis, is obtained from the ZnNNN complex specifically prepared for the NMR assignment.

When dissolved in DMSO, NiNNN has a diamagnetic NMR spectrum, likely due to changes in coordination of the Ni center. However, the NMR spectrum observed in non-coordinating methylene chloride has broad line-shapes and unusual chemical shifts, typical of paramagnetic complexes. Strong magnetic interactions between the NMR active nuclei and unpaired electrons typically lead to significant line broadening and temperature-dependent chemical shifts that occur far outside of the normal range of diamagnetic molecules, making the usual methods of assigning and interpreting NMR spectra inapplicable. In fact, routine structural assignments of

^aDepartment of Chemistry, Yale University, P.O. Box 208107, New Haven, CT 06520-8107, USA. E-mail: robert.crabtree@yale.edu, eric.paulson@yale.edu, steven.konezny@yale.edu, victor.batista@yale.edu

^bEnergy Sciences Institute, Yale University, P.O. Box 27394, West Haven, CT 06516-7394, USA

^cDepartment of Chemistry, University of Ottawa, 10 Marie-Curie, Ottawa, Canada, K1N 6N5

^dCentre for Catalysis Research and Innovation, University of Ottawa, 30 Marie Curie, Ottawa, Canada, K1N 6N5

†Electronic supplementary information (ESI) available. CCDC 926643. For ESI and crystallographic data in CIF or other electronic format see DOI: 10.1039/c3dt50528f

paramagnetic spectra generally remain inaccessible. While the ratios of integrated peak areas can be helpful in making NMR assignments, in most paramagnetic cases including the present study, line broadening induced by the paramagnetic center leads to unreliable peak integration.

Previous paramagnetic studies reported in the literature often demonstrate the assignment of at most two or three proton environments.⁴ In the present work, we demonstrate the assignment and interpretation of the paramagnetic NMR of NiNNN with six proton environments by combining DFT computations with NMR relaxation and variable temperature measurements of chemical-shifts.⁵

Paramagnetic NMR methods have been applied to elucidate structural features in a variety of systems such as metalloproteins,⁶ and metal complexes bound to DNA,⁷ including experiments in the solid state.⁸ Our study of NiNNN complements these earlier studies. Other paramagnetic 5-coordinate Ni complexes with triplet ground states have been reported,^{9,10} including the trigonal bipyramidal pyridine(2,6-diacetimidophenyl)-dithiolate and diselenide complexes,¹¹ a square pyramidal cysteine Ni complex,¹² a complex of a penta-aza macrocyclic ligand,¹³ nickel chelate thioether complexes¹⁴ and complexes of tetradentate ligands with solvent coordination.¹⁵ Therefore, we anticipate that the combined NMR/DFT methodology implemented in this study should be useful to address a variety of other paramagnetic 3d complexes such as five-coordinate nickel complexes^{5,16} inspired by the active site of [Ni-Fe] hydrogenase as in the sulfate reducing bacterium *Desulfovibrio gigas*.¹⁷

Paramagnetic ¹H NMR analysis

The theory of paramagnetic NMR spectroscopy is well established.^{5,18} In paramagnetic molecules, interactions between the nucleus and the unpaired electron spin(s) spread out the observed chemical shifts δ over a much wider range than typically seen for diamagnetic molecules. The local electron cloud around the resonating nucleus still provides an orbital contribution δ_{dia} to the observed chemical shift, although the large magnetic moment induced by the unpaired electron(s) provides a predominant additional contribution given by the temperature-dependent hyperfine shift δ_{HF} .¹⁹

$$\delta(T) = \delta_{\text{dia}} + \delta_{\text{HF}}(T) \quad (1)$$

The orbital contribution is similar to the chemical-shift observed for a diamagnetic analogue molecule (*e.g.*, ZnNNN) and is temperature independent to the extent that the molecular structure is temperature independent. In many cases, the hyperfine shift $\delta_{\text{HF}}(T)$ can be accurately described as the sum of the pseudocontact and Fermi shifts, δ_{pc} and δ_{con} , respectively:

$$\delta_{\text{HF}}(T) = \delta_{\text{pc}}(T) + \delta_{\text{con}}(T) \quad (2)$$

where δ_{pc} is determined by the electron-nuclear *through-space* interactions, typically modeled as the dipolar coupling

between the nuclear magnetic moment and the magnetic moment of the unpaired electron treated as a point dipole.²⁰ Its contribution to the overall hyperfine shift δ_{HF} is most significant when the NMR active nucleus is in close proximity to the paramagnetic center. *Through-bond* electron-nuclear interactions, due to electron spin delocalization onto nuclei that interact with the resonating nucleus, determine the Fermi contact shift.^{21,22}

$$\delta_{\text{con}} = \frac{\mu_0 \mu_B^2 g_e^2 (S+1)}{9k_B T} \rho_{\alpha-\beta} \quad (3)$$

where μ_0 is the vacuum permeability, μ_B is the Bohr magneton, g_e is the free-electron g factor, S is the total spin of the system, k_B is the Boltzmann constant, T is the absolute temperature in K, and $\rho_{\alpha-\beta}$ is the residual spin density of the unpaired electron on the nuclei that interacts with the resonating nucleus. While this treatment is strictly applicable for systems with negligible zero-field splitting (ZFS) and no deviations from Curie behavior (linearity of observed chemical shifts *vs.* $1/T$),⁵ it provides a useful approximation for systems with non-zero ZFS.²³

The relaxation times of NMR-active nuclei are mostly affected by *through-space* dipolar interactions that accelerate the relaxation times, typically determined *via* arrayed 1D NMR techniques. These longitudinal relaxation times $T_{1\text{N}}$ are approximately correlated to the distance r between the resonating nucleus and the paramagnetic center modeled as a point dipole, as follows:

$$\frac{1}{T_{1\text{N}}} = \frac{4S(S+1)\gamma_N^2 g^2 \beta^2 T_{1e}}{r^6} \quad (4)$$

Here, T_{1e} is the electron spin lattice relaxation time that is often treated as a free parameter to be fitted to the observed data since it can be difficult to determine at the temperatures and magnetic fields used in NMR spectroscopy.

In our study of NiNNN, the dependence of the observed $T_{1\text{N}}$ as a function of distance from the paramagnetic center was used to correlate and confirm the DFT-assisted assignment of the paramagnetic NMR spectrum. Variable temperature ¹H NMR data were collected in CD₂Cl₂ on a 500 MHz NMR instrument in the temperature range from -80° to 20 °C. The direct current (dc) magnetic susceptibility measurements were carried out in the temperature range of 2.5–300 K under an applied field of 1000 Oe.

Results and discussion

Fig. 2 shows the dc magnetic susceptibility χT as a function of temperature T in the 2.5–300 K range under an applied field of 1000 Oe. The measured room temperature χT value is 1.34 cm³ K mol⁻¹, which is only slightly higher than the theoretical value of 1.00 cm³ K mol⁻¹ for a mononuclear Ni(II) complex where $g = 2.0$. As the temperature decreases to 30 K, the χT value slightly decreases before rapidly dropping to reach a minimum of 0.28 cm³ K mol⁻¹ at 2.5 K. This behavior is indicative of depopulation of low-lying excited states and/or

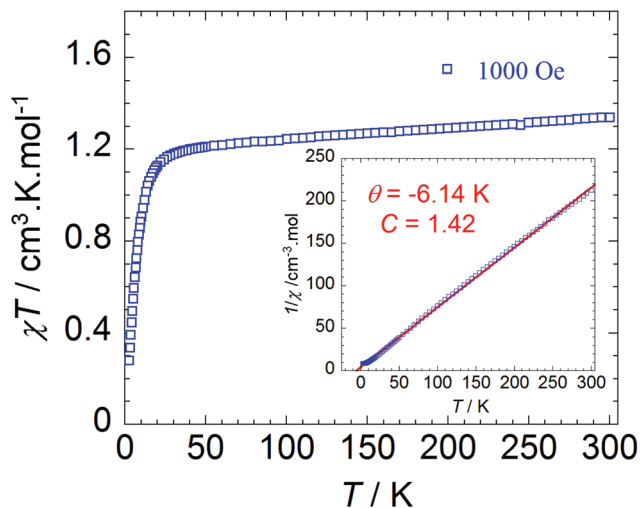


Fig. 2 Temperature dependence of the χT product for the NiNNN complex under an applied dc field of 1000 Oe. *Inset*: Fitting of the $1/\chi$ vs. T plot using the Curie–Weiss law; the red line indicates the fit.

the presence of weak intermolecular antiferromagnetic interactions between the mononuclear complexes. Fitting the $1/\chi$ vs. T plot (Fig. 2, *inset*) to the Curie–Weiss law yields a Curie constant $C = 1.42$ and a Weiss constant $\theta = -6.14$ K, confirming weak intermolecular antiferromagnetic interactions.

The magnetization plots, M vs. H and M vs. H/T , for NiNNN (presented in the ESI; Fig. S1-1 and S1-2†) show a field dependence of the magnetization that does not saturate at low temperatures (2.5 K) and high magnetic fields (up to 7 T) and magnetization curves that are not superimposable on a single master curve indicating the presence of magnetic anisotropy and/or low lying excited states. The obtained data confirm the paramagnetic nature of the five coordinate Ni(II) complex with the expected $S = 1$ spin ground state.

Fig. 3 shows the temperature-dependent ^1H NMR data in CD_2Cl_2 , exhibiting six specific peaks with distinct T -dependent chemical shifts as measured with a 500 MHz NMR instrument.

Fig. 3(b) shows that the chemical shifts change linearly as a function of T^{-1} , consistent with Curie's law, allowing for the DFT assignment of the six proton environments, as described below. DFT methods were used to correlate this linear behavior with the calculated hyperfine term of the chemical shift $\delta_{\text{HF}}(T)$, as obtained according to the residual spin densities of each proton and the orbital contribution estimated by the diamagnetic reference compound (ZnNNN), prepared specifically for the purpose of providing a reliable temperature-independent δ_{dia} .

The newly prepared diamagnetic ZnNNN complex has a trigonal bipyramidal structure (Fig. 4, right), somewhat distorted due to the rigidity of the NNN ligand (.cif file in ESI†). In comparison, the NiNNN complex (Fig. 4, left) has similar metal–ligand distances and angles, although with a geometry closer to square pyramidal. Slight structural differences were also observed in earlier comparisons of Zn and Ni analogs of 4-coordinate species.^{5b} These results indicate that Zn and Ni

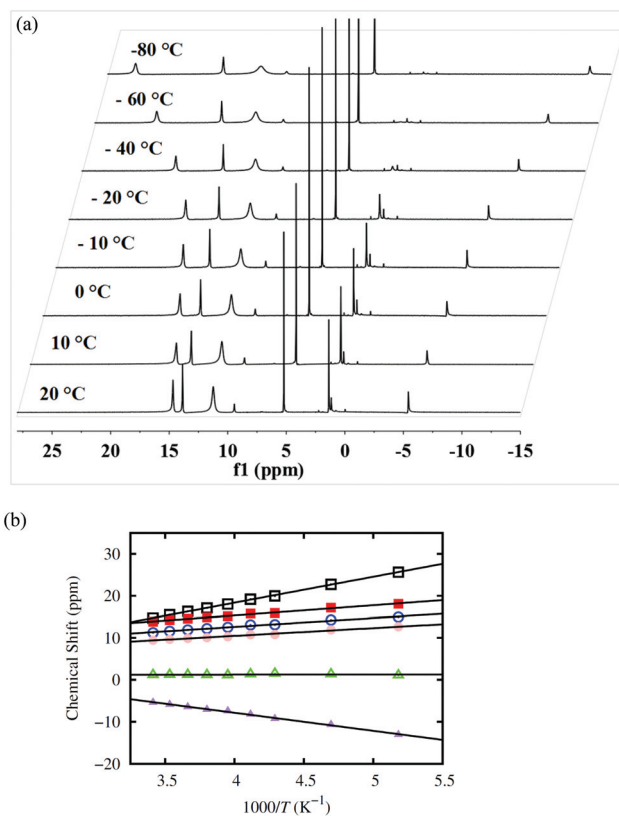


Fig. 3 (a) NiNNN variable temperature ^1H NMR spectra collected in CD_2Cl_2 at 500 MHz and temperatures from -80°C to 20°C as indicated. Peaks labeled **1–6** from the most downfield to the most upfield in decreasing ppm values. (b) Curie behavior of the ^1H NMR chemical shifts shown in panel (a), including peak **1b** (black squares), **2e** (red squares), **3d** (blue circles), **4c** (pink circles), **5a** (green triangles), **6f** (purple triangles).

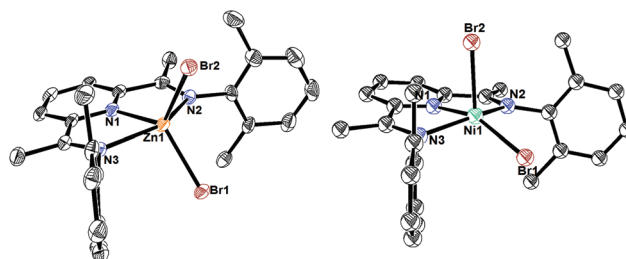


Fig. 4 Comparison of the X-ray structures of NiNNN (left) and ZnNNN (right) complexes. ORTEP plots shown at 40% probability ellipsoids. H atoms are omitted for clarity.

complexes are sufficiently similar to have similar values of δ_{dia} , consistent with DFT calculations (Table 1).

Table 1 shows that the diamagnetic shielding constants calculated at the DFT/UB3LYP/6-311++G(d,p) level of theory are in good agreement with the chemical shifts measured for the diamagnetic reference (deviations between measured and calculated data are less than 0.2 ppm). Having the orbital contribution, our preliminary assignments were made by correlating the computed Fermi contact couplings with the experimental values of δ_{HF} , determined by the slopes of the Curie

Table 1 ^1H NMR assignments for NiNNN, average distances r for isochronous protons obtained from the crystal structure of NiNNN,²⁶ and calculated and experimental values of the diamagnetic δ_{dia} and hyperfine δ_{HF} contributions to the chemical shifts. Experimental δ_{dia} corresponds to the chemical shift of the analogous Zn compound. Calculated δ_{HF} assumes $\delta_{\text{HF}} \approx \delta_{\text{con}}$

Proton	Peak	NiNNN r (Å)	ZnNNN δ_{dia} exp.	NiNNN δ_{dia} calc.	NiNNN $10^{-3}T^*\delta_{\text{HF}}$ exp.	NiNNN $10^{-3}T^*\delta_{\text{HF}}$ calc.
H _a	5	6.44	8.48	8.43	0.02 ± 0.08	−0.94
H _b	1	4.02	8.30	8.37	6.18 ± 0.05	17.94
H _c	4	5.40	2.34	2.26	1.84 ± 0.07	2.05
H _d	3	4.30	2.23	2.04	2.10 ± 0.09	4.88
H _e	2	5.88	7.14	7.27	2.43 ± 0.06	2.36
H _f	6	6.63	7.10	7.22	−4.32 ± 0.09	−4.72

plots (Fig. 3b) for protons far enough from the metal center for dipolar interactions to be small ($\delta_{\text{HF}} \approx \delta_{\text{con}}$). Comparison of experimental δ_{HF} and calculated δ_{con} values in Table 1, with particular attention to the sign of the slope and the metal–proton distance, yields a direct assignment of peaks 2, 4, 5 and 6 to protons H_e, H_c, H_a, and H_f, respectively. The remaining assignments can be made through the analysis of T_1 values, as described below.

Following the preliminary assignment based on calculations of δ_{con} , we turned our attention to the pseudocontact interaction and its measurable effect on the nuclear longitudinal relaxation T_1 since the closer the proton is to the paramagnet, the shorter the relaxation time should be. In order to obtain the *through-space* distances necessary for analysis, we averaged the distances between each isochronous proton in the crystal structure of NiNNN.⁴ The linear correlation between r^6 and the measured relaxation time T_1 (Fig. 5) confirms the existence of dipolar *through-space* interactions according to eqn (4). The data point corresponding to H_a is omitted from this analysis since the experimental peak is overlapped with other signals (making it difficult to obtain accurate integrations) and T_1 is sensitive to slight changes in integration.

The resulting correlation between the proximity of the proton to the paramagnetic center and the observed relaxation

time leads to the assignment of H_b and H_d to peaks 1 and 3, respectively, since they correspond to the shortest measured T_1 values.

In summary, we have successfully assigned the paramagnetic ^1H NMR spectrum of NiNNN by combining temperature-dependent NMR measurements and DFT methods. To the best of our knowledge, this is the first time that paramagnetic NMR of a compound with this level of complexity is fully assigned and characterized. The methodology is simple and general, so it should be useful and applicable for a wide range of systems that permit analysis by paramagnetic NMR and DFT calculations of chemical shifts. The analogous Zn compound provided the diamagnetic reference chemical shifts, essential for the analysis. Assignment of all proton signals, including protons in proximity to the paramagnetic center, was possible on the basis of temperature-dependent chemical shift measurements, observations of T_1 relaxation times, and calculations of diamagnetic shielding constants and isotropic Fermi contact couplings. The analysis of the magnitude of observed relaxation times against distances in the crystal structure allowed a complete assignment of the six significantly broadened ^1H NMR peaks of a redox-active NNN ligand in a Ni^{II} complex.^{2a}

Experimental

All reagents were received from commercial sources and used without further purification unless otherwise specified. Solvents were dried by passage through a column of activated alumina followed by storage under dinitrogen. NMR spectra were recorded on Bruker AMX 500 MHz spectrometers unless otherwise specified. Chemical shifts are reported with respect to a residual internal protio solvent for ^1H . Literature procedures were utilized to synthesize NiNNN.²⁴ Elemental analyses were performed by Robertson Microlit Inc.

NMR data were collected in CD_2Cl_2 unless otherwise noted. T_1 data were collected on a 500 MHz Bruker instrument at -40 °C. The data were worked up using the Bruker Topspin T_1/T_2 relaxation module and MestReNova 5.2.4-3824. Exponential fits and specific delays are available in the ESI.† (d1 = 2s, SW = 50, 64 scans per datapoint). Stacked spectra and delay details are also available in the ESI.†

Variable temperature magnetic susceptibility measurements were obtained using a Quantum Design SQUID

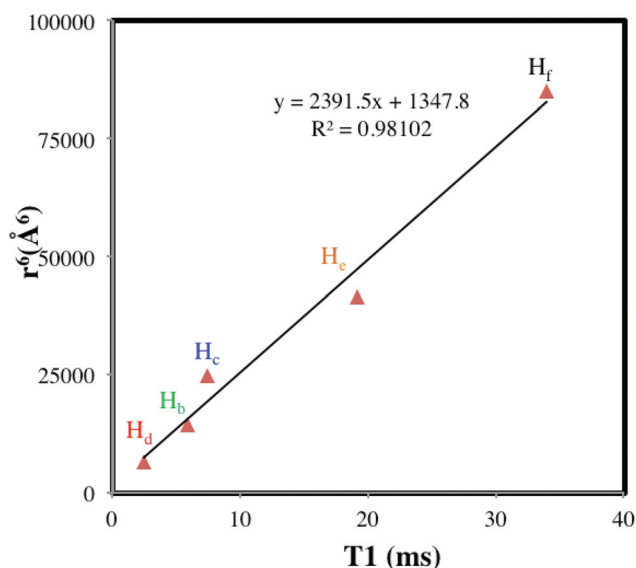


Fig. 5 Plot of r^6 vs. T_1 relaxation for NiNNN. (source data available in S5†).

MPMS-XL7 magnetometer which operates between 1.8 and 300 K for direct current (DC) applied fields up to 7 T. Measurements were performed on a polycrystalline sample of Ni₃NN (16.6 mg). The absence of ferromagnetic impurities was confirmed by measuring the magnetization as a function of field at 100 K. The magnetic data were corrected for the sample holder and diamagnetic contributions from the sample.

Computational methods

Density functional theory calculations were performed using Gaussian 09²⁵ and the B3LYP exchange–correlation functional with unrestricted Kohn–Sham wave functions (UB3LYP). The minimum energy structure of Ni₃NN (Fig. 1, right) was obtained in the gas phase using a mixed basis with the LANL2DZ basis set for Ni and the 6-311++G(d,p) basis set for all other atoms. NMR shielding constants and Fermi-contact terms were calculated using the gauge-independent atomic orbital (GIAO) approach in conjunction with the polarizable continuum model as implemented in Gaussian 09 with a dielectric constant of $\epsilon = 8.93$ (dichloromethane) for the continuum solvating medium. Calculated values of δ_{dia} and $10^{-3}T^*\delta_{\text{HF}}$ reported in Table 1 are an average of isochronous protons, as defined in Fig. 1 (left). A reference chemical shift of 31.77 ppm was used for the calculated values of δ_{dia} for Ni₃NN (Table 1). This value was obtained by minimizing the deviation from the values of δ_{dia} measured for the diamagnetic reference (Table 1) and is in good agreement with a value of 31.97 ppm for tetramethylsilane calculated at the same level of theory and solvent conditions.

Acknowledgements

The work was supported as part of the Center for Electrocatalysis, Transport Phenomena, and Materials (CETM) for Innovative Energy Storage, an Energy Frontier Research Center funded by the U.S. Department of Energy, Office of Science, Office of Basic Energy Sciences under Award Number DE-SC00001055. [OL, RHC for NMR experiments and assignment; KL synthesis of ZNNN; EP help with data collection and analysis; SJK, VSB computation component of assignment; FH, MM Magnetism measurements]. We thank Prof. Jack Faller and Prof. Gary Brudvig for useful discussions. We thank the University of Ottawa, CCRI, NSERC (Discovery and RTI grants); ERA, Vision 2010, CFI, ORF, FFCR. We thank Dr Nathan Schley and Dr Michael Takase for the crystal structure refinement.

References

- 1 R. H. Crabtree, *Energy Environ. Sci.*, 2008, **1**, 134.
- 2 (a) O. R. Luca, S. J. Konezny, J. D. Blakemore, S. Saha, D. M. Colosi, G. W. Brudvig, V. S. Batista and R. H. Crabtree, *New J. Chem.*, 2012, **36**, 1149–1152; (b) O. R. Luca and R. H. Crabtree, *Chem. Soc. Rev.*, 2013, **42**, 1440–1459; (c) O. R. Luca, J. D. Blakemore, J. M. Praetorius, T. J. Schmeier, G. B. Hunsinger, V. S. Batista, G. W. Brudvig, N. Hazari and R. H. Crabtree, *Inorg. Chem.*, 2012, **51**, 8704–8709.
- 3 (a) L. Sacconi, *Pure Appl. Chem.*, 1968, **17**, 95–127; (b) I. Morassi, I. Bertini and L. Sacconi, *Coord. Chem. Rev.*, 1973, **11**, 343–402; (c) L. Sacconi, G. P. Speroni and R. Morassi, *Inorg. Chem.*, 1968, **7**, 1521–1525.
- 4 (a) T. O. Pennanen and J. Vaara, *Phys. Rev. Lett.*, 2008, **100**, 133002; (b) H. Liimatainen, T. O. Pennanen and J. Vaara, *Can. J. Chem.*, 2009, **87**, 954; (c) J. Mao, Y. Zhang and E. Oldfield, *J. Am. Chem. Soc.*, 2002, **124**, 13911; (d) R. Knorr, H. Hauer, A. Weiss, H. Polzer, F. Ruf, P. Löw, P. Dvortsák and P. Böhrer, *Inorg. Chem.*, 2007, **46**, 8379; (e) P. Fernández, H. Pritzkow, J. Carbó, P. Hofmann and M. Enders, *Organometallics*, 2007, **26**, 4402; (f) M. Kruck, D. C. Sauer, M. Enders, H. Wadeplahl and L. H. Gade, *Dalton Trans.*, 2011, **40**, 10406.
- 5 (a) L. Bertini and C. Luccinat, *Coord. Chem. Rev.*, 1996, **150**, 1–296; (b) P. Roquette, A. Maronna, M. Reinmuth, E. Kaifer, M. Enders and H.-J. Himmel, *Inorg. Chem.*, 2011, **50**, 1942–1955; (c) T. E. Manchonkin, M. W. Westler and J. L. Markley, *Inorg. Chem.*, 2005, **44**, 779–797.
- 6 I. Bertini, O. Turano and A. J. Vila, *Chem. Rev.*, 1993, **93**, 2833–2932.
- 7 P. K. Bhattacharya, H. J. Lawson and J. K. Barton, *Inorg. Chem.*, 2003, **42**, 8811–8817.
- 8 S. Ballayssac, I. Bertini, A. Bhaumik, M. Lelli and C. Luchinat, *Proc. Natl. Acad. Sci. U. S. A.*, 2008, **105**, 17284–17289.
- 9 E. W. Abel, R. J. Puddephatt, F. G. A. Stone and G. Wilkinson, *Comprehensive organometallic chemistry II: a review of the literature, 1982–1994*, Pergamon, 1995.
- 10 S. C. Davies, D. J. Evans, D. L. Hughes, S. Longhurst and J. R. Sanders, *Chem. Commun.*, 1999, 1935–1936.
- 11 C. A. Marganian, H. Vazir, N. Baidya, M. M. Olmstead and P. K. Mascharak, *J. Am. Chem. Soc.*, 1995, **117**, 1584–1594.
- 12 S. A. Ross and C. J. Burrows, *Inorg. Chem.*, 1998, **37**, 5358–5363.
- 13 E. Kimura and R. Machida, *J. Chem. Soc., Chem. Commun.*, 1984, 499–500.
- 14 A. J. Blake, R. O. Gould, M. A. Halcrow and M. Schröder, *J. Chem. Soc., Dalton Trans.*, 1993, 2909–2920.
- 15 (a) H. Pannemann, S. Wassmann, J. Wilken, H. Gröger, S. Wallbaum, M. Kossenjans, D. Hasse, W. Saak, S. Pohl and J. Martens, *J. Chem. Soc., Dalton Trans.*, 2000, 2467–2470; (b) M. Bröring, S. Prikhodovski and C. D. Brandt, *J. Chem. Soc., Dalton Trans.*, 2002, 4213–4218.
- 16 E. W. Abel, R. J. Puddephatt, F. G. A. Stone and G. Wilkinson, *Comprehensive organometallic chemistry II: a review of the literature 1982–1994*, Pergamon, 1995.
- 17 M.-H. Volbeda, C. Charon, E. C. Piras, M. Hatchikian, M. Frey and J. C. Fontecilla-Camps, *Nature*, 1995, **373**, 580.
- 18 (a) *NMR of Paramagnetic Molecules*, ed. G. N. La Mar, W. DeW. Horrocks Jr. and R. H. Holm, Academic Press,

- New York, 1973; (b) F. H. Köhler, *Magnetism: Molecules to Materials*, ed. J. S. Miller, M. Drillon, Wiley-VCH, Weinheim, 2001, pp. 379–430; (c) I. Bertini, C. Luchinat and G. Parigi, *Prog. Nucl. Magn. Reson. Spectrosc.*, 2002, **40**, 249; (d) I. Bertini, C. Luchinat, G. Parigi and R. Pierattelli, *Chem-BioChem*, 2005, **6**, 1536; (e) F. Rastrelli and A. Bagno, *Chem.-Eur. J.*, 2009, **15**, 7990; (f) M. Kaupp and F. H. Köhler, *Coord. Chem. Rev.*, 2009, **253**, 2376.
- 19 (a) I. Bertini, C. Luchinat and G. Parigi, *Solution NMR of Paramagnetic Molecules- Applications to metalloproteins and Models*, Elsevier, Amsterdam, 2001; (b) J. P. Jesson, *NMR of Paramagnetic Molecules- Principles and Applications*, Academic Press, New York, London, 1973.
- 20 Pseudocontact shift arises from the averaging of the δ_{pc} due to tumbling in solution.
- 21 R. S. Drago, *Physical Methods for Chemists*, Surfside Scientific Publishers, 2nd edn, 1997.
- 22 L. Que Jr., *Physical Methods in Bioinorganic Chemistry Spectroscopy and Magnetism*, University Science Books, 2000.
- 23 (a) M. J. Kurland and B. R. McGarvey, *J. Magn. Reson.*, 1970, **2**, 286–381; (b) P. Rocquette, A. Maronna, A. Peters, E. Kaifer, H.-J. Himmel, C. Hauf, V. Herz, E.-W. Scheidt and W. Scherer, *Chem.-Eur. J.*, 2010, **16**, 1336–1350.
- 24 H. Suzuki, S. Matsumura, Y. Satoh, K. Sogoh and H. Yasuda, *React. Funct. Polym.*, 2004, 77–91.
- 25 T. D. Manuel and J.-U. Rohde, *J. Am. Chem. Soc.*, 2009, **131**, 15582–15583.
- 26 M. J. Frisch, *et al.* *GAUSSIAN 09 (Revision A.1)*, Gaussian, Inc., Wallingford CT, 2009. See the ESI† for the complete reference.